Atmos. Meas. Tech., 5, 1841–1846, 2012
www.atmos-meas-tech.net/5/1841/2012/
doi:10.5194/amt-5-1841-2012

Atmospheric Measurement Techniques

Direct comparisons of GOMOS and SAGE III NO_3 vertical profiles

J. Hakkarainen[1,2], **J. Tamminen**[1], **J. R. Moore**[3], **and E. Kyrölä**[1]

[1]Finnish Meteorological Institute, Earth Observation, Helsinki, Finland
[2]Lappeenranta University of Technology, Lappeenranta, Finland
[3]Science Systems and Applications, Inc., Hampton, Virginia, USA

Correspondence to: J. Hakkarainen (janne.hakkarainen@fmi.fi)

Received: 8 December 2011 – Published in Atmos. Meas. Tech. Discuss.: 13 February 2012
Revised: 21 June 2012 – Accepted: 10 July 2012 – Published: 31 July 2012

Abstract. In this paper, we present the first global comparisons between the two unique satellite-borne data sets of nitrogen trioxide (NO_3) vertical profiles retrieved from the GOMOS (Global Ozone Monitoring by the Occultation of Stars) stellar occultations and the SAGE III (Stratospheric Aerosol and Gas Experiment) lunar occultations. The comparison results indicate that between the altitudes 25 km and 45 km the median difference between these two data sets is within ±25 %. The study of zonal median profiles shows that the climatologies calculated from GOMOS and SAGE III profiles are comparable and represent the same features in all latitude bands. No clear systematic differences are observed. The median profiles are closest in the tropics and slightly deviating at high latitudes.

1 Introduction

The radical nitrate NO_3 is important in the stratospheric nighttime photochemistry. It is chemically coupled to nitrogen oxides ($NO_x = NO + NO_2$), whose reactions in the middle atmosphere form the primary catalytic ozone destruction cycle (Marchand et al., 2004). NO_3 has strong diurnal variations, and during sunrise and sunset photolysis destroys NO_3 extremely quickly in the presence of sunlight. During the nighttime, in the absence of heterogeneous processes, the NO_3 chemistry scheme is believed to be relatively simple with three reactions:

$$NO_2 + O_3 \rightarrow NO_3 + O_2 \quad \text{(R1)}$$

$$NO_3 + NO_2 + M \rightarrow N_2O_5 + M \quad \text{(R2)}$$

$$N_2O_5 + M \rightarrow NO_3 + NO_2 + M \quad \text{(R3)}$$

NO_3 is mainly produced by Reaction (R1) of NO_2 and O_3. The sink of NO_3 is the Reaction (R2) with NO_2 which produces N_2O_5, which during the polar winter and spring reacts on the surface of stratospheric sulphate aerosol heterogeneously to form HNO_3 and polar stratospheric clouds (Amekudzi et al., 2005). The thermal decomposition of N_2O_5 (Reaction R3) is an additional source of NO_3 (Marchand et al., 2004).

Historically, NO_3 has been observed by ground-based lunar measurements, and the first measurements of NO_3 were published by Noxon et al. (1978). In addition to ground-based measurements, balloon-borne measurements to observe the vertical structures have been made using stellar and lunar occultations (Naudet et al., 1981; Renard et al., 1996). Recently, NO_3 slant-column densities have been observed through sunrise and sunset using limb-scattered solar light measured by OSIRIS (McLinden and Haley, 2008).

Due to the strong diurnal variation of NO_3, in practice existing only during nighttime and being undetectable during daytime, there are only a few data sets of satellite-borne NO_3 profiles available. The GOMOS (Global Ozone Monitoring by the Occultation of Stars) instrument has provided a long data set of simultaneous NO_2 and NO_3 observations since August 2002 (Hauchecorne et al., 2005; Kyrölä et al., 2010a). While GOMOS uses stellar light as a light source to measure the vertical distributions in the atmosphere, SAGE III (Stratospheric Aerosol and Gas Experiment) and SCIAMACHY (SCanning Imaging Absorption spectroMeter for Atmospheric CHartographY) employ the lunar occultation technique to observe NO_3.

The strong diurnal variation makes the validation challenging, and many previous validations of the satellite-borne NO_3 profiles include models and/or a chemical data

Published by Copernicus Publications on behalf of the European Geosciences Union.

assimilation schemes (e.g. Marchand et al., 2004; Amekudzi et al., 2007). In the study of Marchand et al. (2004), the self-consistency of GOMOS NO_3, NO_2 and O_3 was verified. Their results also indicated that there is no substantial bias in GOMOS NO_3 data. In the study of Renard et al. (2008), four GOMOS NO_3 profiles were compared against balloon-borne observations as a "one-shot" validation exercise.

To our knowledge, this is the first paper where the satellite-borne NO_3 profiles are directly compared with each other.

2 Data sets and methods

2.1 GOMOS data

The GOMOS (Global Ozone Monitoring by the Occultation of Stars) instrument was launched on 1 March 2002 by the European Space Agency on board the ENVISAT platform (Bertaux et al., 2010). Since August 2002, GOMOS has provided more than 850 000 individual vertical profiles of ozone, NO_2, NO_3 and other species. About half of the occultations are made during nighttime. In the beginning of the mission, the instrument made about 400–500 occultations in a day, but, due to the instrumental problems leading to the reduced viewing angle, the number of occultations has been about 200–300 since January 2005. GOMOS nighttime observations are made during the ascending path of ENVISAT, and the local time is approximately equal to the local hour of the ascending node, 22:00 LT (Bertaux et al., 2010). GOMOS tangent point local times cover 1.5 h at the Equator and 3 h at mid-latitudes (Kyrölä et al., 2010a).

The GOMOS inversion has been split in two parts: the spectral inversion and the vertical inversion (Kyrölä et al., 2010b). In the first part, horizontally integrated line densities of O_3, NO_2, NO_3 and aerosols are retrieved simultaneously using a combination of absolute and differential cross sections. In the second part, NO_3 profiles are retrieved from these horizontally integrated line densities at different tangent altitudes. In the latter part, Tikhonov regularization is applied to compensate low signal-to-noise ratio. The vertical resolution of the NO_3, with the current regularization parameter, is 4 km while the sampling resolution (which corresponds to both tangent height resolution and the vertical grid of the product) is smaller (0.5–1.7 km). Besides a smoothing requirement used in Tikhonov regularization, the GOMOS inversion does not use any a priori information of NO_3 profiles.

As GOMOS uses stellar light as a light source, the quality of the measurements and the observations varies from star to star. In the study of Tamminen et al. (2010), GOMOS data were characterized. They concluded that NO_3 can be observed in the 25–45 km altitude range with a precision of 20–40 % with the bright and medium bright stars, and noted also that the cool stars are slightly more favorable for the NO_3 retrieval. In this work, we study only the NO_3 profiles that have been retrieved using stars brighter than 1.9 magnitude and cooler than 15 000 K. We have also screened the GOMOS data so that the solar zenith angle is higher than 107°. We use the GOMOS data version IPF 5.0.

In Fig. 1, we show an example of the GOMOS spectral fit at 40 km and the mean GOMOS spectral fit calculated from the tangent heights between 30 and 45 km. In Fig. 1, the NO_3 absorption features located at 623 nm and 662 nm are clearly visible. The GOMOS star used in this occultation is Alpha Carinae (GOMOS star number 2), which is optimal for measuring NO_3. It is a bright and cool star, and thus the signal-to-noise ratio around the NO_3 absorption bands is high. The GOMOS spectral fitting window is from 248 nm to 690 nm, but in Fig. 1 we have concentrated on area where the NO_3 absorption features are located.

2.2 SAGE III data

SAGE III continued the heritage of SAGE I (1979–1981) and SAGE II (1984–2005) by measuring ozone, nitrogen dioxide, water vapor, and aerosol extinctions by solar occultation technique (McCormick et al., 1989) and additionally performed new nocturnal measurements of ozone, NO_2, and NO_3 using lunar occultation technique (SAGE III ATBD Team, 2002). SAGE III was launched 10 December 2001 on board a Russian Meteor-3M spacecraft, and it recorded data between 7 May 2002–26 October 2005 in lunar occultation mode.

The current SAGE III lunar data set version 3.0 includes 583, 717, 959 and 302 vertical profiles for the years 2002, 2003, 2004 and 2005, respectively. The v3.0 data set contains nocturnal vertical profiles of ozone, NO_2, and NO_3 with near-global coverage. Approximately 32 % of SAGE III lunar measurements occurred between 23:00 and 24:00 local solar time at the tangent point, and approximately 49 % of the measurements occurred in polar regions ($|\text{latitude}| > 60°$). Measurements were attempted when the lunar phase was 40 % or greater and the solar zenith angle greater than 95 degrees. Algorithms for altitude registration, refraction, and data binning were derived using techniques similar to the SAGE II (Chu et al., 1989) and SAGE III solar processing (Chu and Veiga, 1998). The gas species retrieval algorithms were developed prior to launch using a complex forward simulation model. The simulation incorporated a solar spectrum over the SAGE III wavelengths reflected by a modeled lunar disk with variable albedo, ray tracing through the atmosphere, and the effects of Rayleigh scattering and absorption by molecular gases and aerosols. Briefly, the retrieval procedure used a differential optical absorption spectroscopy algorithm (Platt et al., 1979) to compute line-of-sight column densities of gas species and then performed an inversion using an onion peel algorithm to compute number density concentrations.

The vertical resolution of the SAGE III NO_3 profiles is 1 km, and the data are given on a 0.5 km fixed grid between

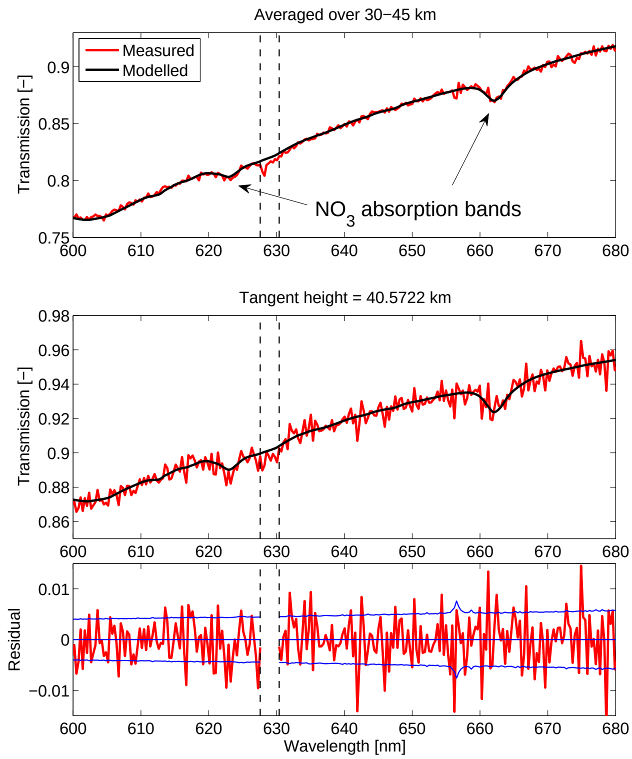

Fig. 1. An example of the GOMOS spectral fit. Uppermost panel shows GOMOS mean spectral fit calculated from the tangent heights between 30 and 45 km. Middle panel shows spectral fit at 40 km, and the lowermost panel is the residual at 40 km. The example is the same as in Fig. 4. NO_3 absorption features are clearly visible. Note that in the GOMOS Level 2 processing the spectral range 627.9–630.1 nm, covering the red line of atomic oxygen and O_2 absorption band, has been flagged and this area is not used in the retrieval (Kyrölä et al., 2010b; Tamminen et al., 2010).

20–60 km. The errors associated with the SAGE III NO_3 observations are provided in the data products and are 20–50 % between 25 km and 45 km. For a detailed description of the instrument, lunar processing algorithms, and cross section data, see SAGE III ATBD Team (2002). In this study, SAGE III data have been screened, so that the solar zenith angle is higher than 107°.

2.3 Collocations and comparisons

These two data sets provide unique information on the night-time NO_3 profiles measured from the Earth's limb. Temporal overlap of the data sets starts in August 2002 and continues until the end of 2005. Still, finding suitable collocations between GOMOS and SAGE III is quite difficult, because the two data sets are not homogeneously distributed (see Fig. 2).

In practice, we need to find a compromise between spatiotemporal limits and statistical representativeness. In order to find matches between GOMOS and SAGE III, we set the maximum latitudinal and longitudinal difference to be 2 and

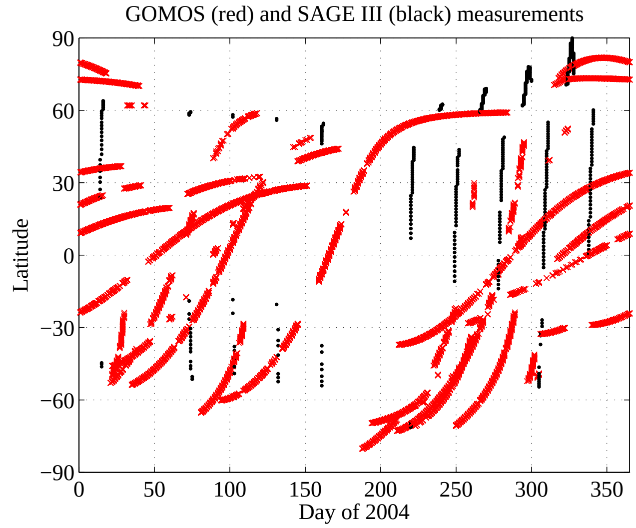

Fig. 2. GOMOS (red) and SAGE III (black) measurements in the year 2004. The GOMOS data have been screened, so that the solar zenith angle is higher than 107° and the stars used are brighter than 1.9 magnitude and cooler than 15 000 K. The SAGE III data have been screened, so that the solar zenith angle is higher than 107°.

5 degrees, respectively. For the temporal difference, we allowed the measurements to be 24 h away from each other, and at the same time set the local hour difference to be less than 2 h. With these criteria, we found 5, 23 and 8 collocated pairs for the years 2002, 2003 and 2004, respectively. For the year 2005, we did not find any matches, mainly due to the fact that SAGE III measured most of its data during a time when GOMOS was suffering from a technical anomaly. If we allow the temporal difference to be one week, still demanding the local hour difference to be less than 2 h, we can find 115 matches instead of 36. In cases where multiple GOMOS matches were found to an individual SAGE III profile, we selected the one that had the smallest time difference. The spatial distribution of these 115 matches is shown in Fig. 3. When 36 collocations are considered, the mean local time difference (GOMOS-SAGE III) is 18 min. When 115 collocations are considered, the mean difference is 7 min.

For statistical analysis, we use a symmetrically normalized GOMOS to SAGE III difference defined as

$$f(g,s) = 200 \times \frac{g-s}{g+s}\,[\%], \tag{1}$$

where g is GOMOS and s is SAGE III. Because GOMOS and SAGE III profiles possess different vertical resolutions, GOMOS averaging kernels are applied to the SAGE III profiles.

The expected variance of the difference (Eq. 1) is approximated by

$$\sigma_f^2 \approx \left|\frac{\partial f}{\partial g}\right|^2 \sigma_g^2 + \left|\frac{\partial f}{\partial s}\right|^2 \sigma_s^2, \tag{2}$$

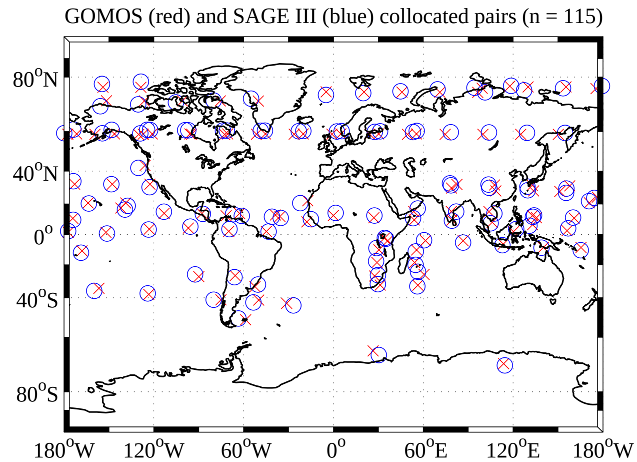

Fig. 3. Spatial distribution of 115 collocated GOMOS-SAGE III pairs (red cross and blue ring) from the years 2002–2004.

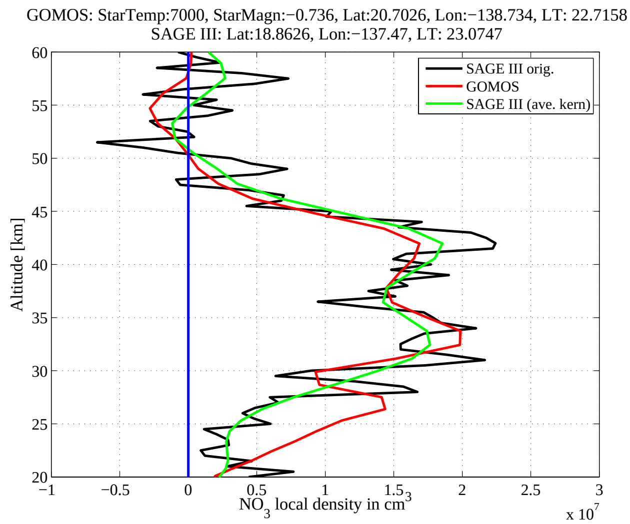

Fig. 4. An individual match between GOMOS and SAGE III showing good agreement. SAGE III profile is plotted before and after the GOMOS averaging kernel was applied. Figure 4 illustrates two-peaked NO_3 profile.

where σ_g and σ_s are the error estimates reported by GOMOS and SAGE III products, respectively. Eq. (2) makes the standard assumption that GOMOS and SAGE III errors are uncorrelated.

3 Results

Herein, we seek to verify the NO_3 measurement accuracies by the direct comparison of GOMOS and SAGE III NO_3 observations.

In Fig. 4 an individual match, illustrating a two-peaked NO_3 profile and showing good agreement between the products, is shown. SAGE III profile is plotted before and after the application of the GOMOS averaging kernel. The example is the same as in Fig. 1.

In Fig. 5, we show the statistics calculated from 36 collocated pairs found from the years 2002–2004. The black solid line is the median of the individual differences, and the black dashed lines correspond to median $\pm$ interquartile deviations. The green horizontal lines represent the 95 % confidence limits ($\pm$ standard error of the mean $\times$ 1.96). For calculating the mean and standard deviation, we neglected the differences where the distance between the value and the median value is higher than $3 \times 1.4826\times$ the median absolute deviation in order to exclude clear outliers. This is approximately the same as rejecting the data outside 3σ limits.

From Fig. 5, we observe quite large deviations and median values oscillating between $\pm$25 %. We can observe a positive bias pattern of some 10 % below 40 km. It is however small compared to the variability. Above 50 km, the median of GOMOS to SAGE III differences increases up to 100 %. These findings are also valid for the years 2003 and 2004 separately. For the year 2002, the structure of the differences is very noisy, mainly due to the fact that we have only 5 collocated pairs (not shown).

In Fig. 5 we also show the mean $\pm$ square root of the median of the individual variances as defined in Eq. (2). When these blue dashed lines are compared against the mean $\pm$ standard deviation (the green dashed lines), we note that the expected errors of the differences are consistent with the observed differences around 40 km, where NO_3 typically peaks. The uncertainties are underestimated below 33 km and overestimated above 42 km.

The statistics from 115 collocated pairs, where the temporal difference is allowed to be one week, are shown in Fig. 6. Again, we can observe a small positive bias of some 10 % below 40 km. From the interquartile deviation, we can clearly see that the spread between the observations starts growing below 30 km and above 45 km. One can observe that the general structures of the medians in Figs. 5 and 6 are similar. We can also see in Fig. 6 that the expected and observed errors are consistent with each other between the altitudes 33 km and 42 km.

In addition to the differences of the collocated pairs, we also compared the zonal medians in different latitude bands in 2004. In order to make these zonal medians more comparable, we concentrated on three month periods where the distributions inside the latitude bands are closest. Based on Fig. 2 for latitude band 60° S–30° S, we selected months 3–5 and for other latitude bands, we selected months 10–12. For the latitude band 90° S–60° S, we selected only one month (October) because after the screening there were only 6 SAGE III profiles.

The results from these six different latitude bands are shown in Fig. 7. We can see similarities with these profiles. In the tropics, the profiles are almost identical and they deviate slightly at high latitudes, while still representing the same

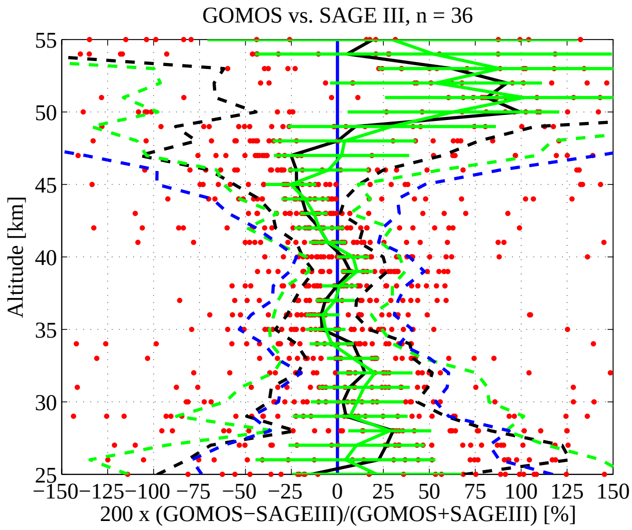

Fig. 5. The statistics of the collocated GOMOS-SAGE III pairs from the years 2002–2004. The black solid line is the median of the individual differences, and the black dashed lines correspond to median ± interquartile deviation. The green solid line is the median filtered mean, and the green horizontal lines represent its 95 % confidence limits. The green dashed lines correspond to mean ± standard deviation, and the blue dashed lines correspond to mean ± square root of the median variance as defined in Eq. (2).

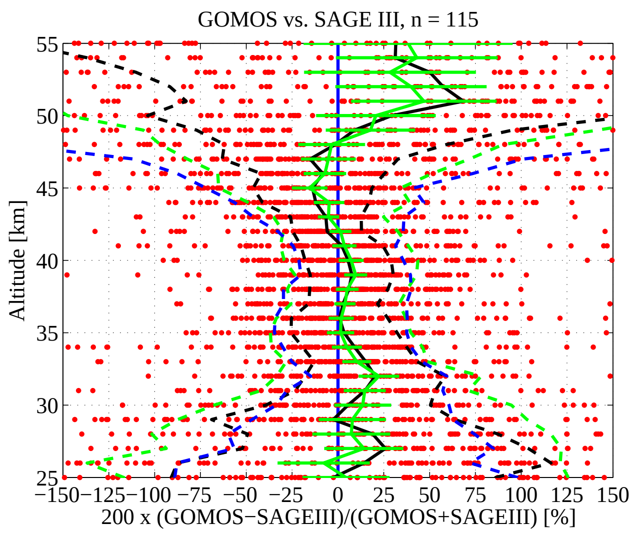

Fig. 6. Same as Fig. 5., except the temporal difference between the measurements is allowed to be as much as one week.

features. We must note that the number of profiles (see the caption of Fig. 7) that is used to calculate the medians is far from equal. Also, the temporal and spatial sampling of the observations varies, although we have concentrated on areas where the distributions are closest. Still, these comparisons confirm that GOMOS and SAGE III nighttime NO_3 climatologies agree well with each other and we do not observe any clear systematic differences between them.

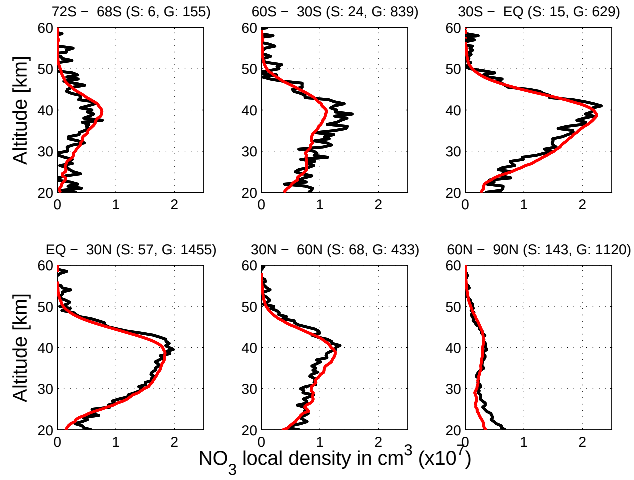

Fig. 7. GOMOS (red) and SAGE III (black) zonal medians in six different latitude bands in 2004. The zonal medians are calculated from three month periods where the spatial and temporal distributions of the measurements inside the latitude band are closest. For latitude band 90° S–60° S, the median is calculated only from one month period (October). The numbers after S and G in titles indicate from how many profiles the median was calculated for SAGE III and GOMOS, respectively.

4 Conclusions and remarks

In this work, we compared GOMOS and SAGE III NO_3 vertical profile data sets, retrieved using stellar and lunar occultation techniques, respectively. Statistical analysis of the limited amount of collocated pairs indicates a good overall agreement between GOMOS and SAGE III. Between the altitudes 25 km and 45 km, the median difference between these two data sets is within ±25 %. From the zonal median profiles, we can see reasonable agreement, showing that the climatological median profiles are comparable. The agreement is at its best in the tropics and slightly worse in other latitude bands. We expect that the better agreement in the tropics is due to more stable atmospheric conditions and more equal sampling of the instruments.

The expected error values of the differences based on the error estimates reported in the data products are consistent with the observed standard deviations between the altitudes 33 km and 42 km. Below 33 km, the observed standard deviations are underestimated. We expect that one reason for this is that the reported GOMOS error estimates are too low. In the next processing version (IPF 6.01), the GOMOS error estimates are expected to be improved and slightly higher for NO_3.

It is worth noting that, despite the noise and other limitations, these two data sets are the only publicly available data sets of NO_3 vertical profiles, leaving GOMOS the sole data set since 2005, when the last SAGE III data were recorded. Vertical profiles of NO_3 are also retrieved from ENVISAT/ SCIAMACHY lunar occultations (Amekudzi et al., 2005), but unfortunately the limited scientific data set did not provide useful information (no collocations found) for comparison with the GOMOS NO_3 vertical profiles. A copy of the SAGE III instrument will be deployed on the International Space Station (ISS) in 2014. It will continue to record data in the lunar occultation mode, and hence it will provide NO_3 vertical profiles.

Acknowledgements. The authors would like to thank the GOMOS and SAGE III teams for providing the data. This work is partly supported by Academy of Finland's MIDAT project. Mr. Moore is supported by the NASA Contract NNL11AA00B through Science Systems and Applications, Inc. The SAGE III data sets are publicly available through the NASA Langley Atmospheric Science Data Center (ASDC). The GOMOS data sets are available via ESA website and registration is required.

Edited by: C. von Savigny

References

Amekudzi, L. K., Sinnhuber, B.-M., Sheode, N. V., Meyer, J., Rozanov, A., Lamsal, L. N., Bovensmann, H., and Burrows, J. P.: Retrieval of stratospheric NO_3 vertical profiles from SCIAMACHY lunar occultation measurement over the Antarctic, J. Geophys. Res., 110, D20304, doi:10.1029/2004JD005748, 2005.

Amekudzi, K. L., Bramstedt, K., Bracher, A., Rozanov, A., Bovensmann, H., and Burrows, J. P.: SCIAMACHY solar and lunar occultation: Validation of ozone, NO_2, and NO_3 profiles, in: Proc. of the Third Atmospheric Chemistry Validation of ENVISAT (ACVE-3), SP-642, ESA Publication Division, 2007.

Bertaux, J. L., Kyrölä, E., Fussen, D., Hauchecorne, A., Dalaudier, F., Sofieva, V., Tamminen, J., Vanhellemont, F., Fanton d'Andon, O., Barrot, G., Mangin, A., Blanot, L., Lebrun, J. C., Pérot, K., Fehr, T., Saavedra, L., Leppelmeier, G. W., and Fraisse, R.: Global ozone monitoring by occultation of stars: an overview of GOMOS measurements on ENVISAT, Atmos. Chem. Phys., 10, 12091–12148, doi:10.5194/acp-10-12091-2010, 2010.

Chu, W. P. and Veiga, R. E.: SAGE III/EOS, in: Proceedings of SPIE, 3501, 52–50, 1998.

Chu, W. P., McCormick, M. P., Lenoble, J., Brogniez, C., and Pruvost, P.: SAGE II inversion algorithm, J. Geophys. Res., 94, 8339–8351, 1989.

Hauchecorne, A., Bertaux, J.-L., Dalaudier, F., Cot, C., Lebrun, J.-C., Bekki, S., Marchand, M., Kyrölä, E., Tamminen, J., Sofieva, V., Fussen, D., Vanhellemont, F., Fanton d'Andon, O., Barrot, G., Mangin, A., Théodore, B., Guirlet, M., Snoeij, P., Koopman, R., Saavedra de Miguel, L., Fraisse, R., and Renard, J.-B.: First simultaneous global measurements of nighttime stratospheric NO_2 and NO_3 observed by Global Ozone Monitoring by Occultation of Stars (GOMOS)/Envisat in 2003, J. Geophys. Res., 110, D18301, doi:10.1029/2004JD005711, 2005.

Kyrölä, E., Tamminen, J., Sofieva, V., Bertaux, J. L., Hauchecorne, A., Dalaudier, F., Fussen, D., Vanhellemont, F., Fanton d'Andon, O., Barrot, G., Guirlet, M., Fehr, T., and Saavedra de Miguel, L.: GOMOS O_3, NO_2, and NO_3 observations in 2002–2008, Atmos. Chem. Phys., 10, 7723–7738, doi:10.5194/acp-10-7723-2010, 2010a.

Kyrölä, E., Tamminen, J., Sofieva, V., Bertaux, J. L., Hauchecorne, A., Dalaudier, F., Fussen, D., Vanhellemont, F., Fanton d'Andon, O., Barrot, G., Guirlet, M., Mangin, A., Blanot, L., Fehr, T., Saavedra de Miguel, L., and Fraisse, R.: Retrieval of atmospheric parameters from GOMOS data, Atmos. Chem. Phys., 10, 11881–11903, doi:10.5194/acp-10-11881-2010, 2010b.

Marchand, M., Bekki, S., Hauchecorne, A., and Bertaux, J.-L.: Validation of the self-consistency of GOMOS NO_3, NO_2 and O_3 data using chemical data assimilation, Geophys. Res. Lett., 31, L10107, doi:10.1029/2004GL019631, 2004.

McCormick, M. P., Zawodny, J. M., Veiga, R. E., Larsen, J. C., and Wang, P. H.: An overview of sage I and II ozone measurements, Planet. Space Sci., 37, 1567–1586, doi:10.1016/0032-0633(89)90146-3, 1989.

McLinden, C. A. and Haley, C. S.: Odin/OSIRIS observations of stratospheric NO_3 through sunrise and sunset, Atmos. Chem. Phys., 8, 5529–5534, doi:10.5194/acp-8-5529-2008, 2008.

Naudet, J. P., Huguenin, D., Rigaud, P., and Cariolle, D.: Stratospheric observations of NO_3 and its experimental and theoretical distribution between 20 and 40 km, Planet. Space Sci., 29, 707–712, 1981.

Noxon, J. F., Norton, R. B., and Henderson, W. R.: Observation of atmospheric NO_3, Geophys. Res. Lett., 5, 675–678, 1978.

Platt, U., Perner, D., and Pätz, H.: Simultaneous Measurement of Atmospheric CH_2O, O_3, and NO_2 by Differential Optical Absorption, J. Geophys. Res., 84, 6329–6335, 1979.

Renard, J.-B., Pirre, M., Robert, C., Moreau, G., Huguenin, D., and Russell III, J. M.: Nocturnal vertical distribution of stratospheric O_3, NO_2 and NO_3 from balloon measurements, J. Geophys. Res., 101, 28793–28804, doi:10.1029/96JD02012, 1996.

Renard, J.-B., Berthet, G., Brogniez, C., Catoire, V., Fussen, D., Goutail, F., Oelhaf, H., Pommereau, J., Roscoe, H. K., Wetzel, G., Chartier, M., Robert, C., Balois, J., Verwaerde, C., Auriol, F., François, P., Gaubicher, B., and Wursteisen, P.: Validation of GOMOS-Envisat vertical profiles of O_3, NO_2, NO_3, and aerosol extinction using balloon-borne instruments and analysis of the retrievals, J. Geophys. Res., 113, A02302, doi:10.1029/2007JA012345, 2008.

SAGE III ATBD Team: SAGE III Algorithm Theoretical Basis Document (ATBD) Solar and Lunar Algorithm, LaRC 475-00-109, Tech. rep., NASA Langley Res. Cent., Version 2.1, available at: http://eospso.gsfc.nasa.gov/eos_homepage/for_scientists/atbd/viewInstrument.php?instrument=14, 2002.

Tamminen, J., Kyrölä, E., Sofieva, V. F., Laine, M., Bertaux, J.-L., Hauchecorne, A., Dalaudier, F., Fussen, D., Vanhellemont, F., Fanton-d'Andon, O., Barrot, G., Mangin, A., Guirlet, M., Blanot, L., Fehr, T., Saavedra de Miguel, L., and Fraisse, R.: GOMOS data characterisation and error estimation, Atmos. Chem. Phys., 10, 9505–9519, doi:10.5194/acp-10-9505-2010, 2010.